ORIGINAL ARTICLE

A transcriptomic study suggesting human iPSC-derived hepatocytes potentially offer a better in vitro model of hepatotoxicity than most hepatoma cell lines

Xiugong Gao · Yitong Liu

Abstract Hepatocytes derived from human induced pluripotent stem cells (iPSCs) hold great promise as an in vitro liver model by virtue of their unlimited long-term supply, stability and consistency in functionality, and affordability of donor diversity. However, the suitability of iPSC-derived hepatocytes (iPSC-Heps) for toxicology studies has not been fully validated. In the current study, we characterized global gene expression profiles of iPSC-Heps in comparison to those of primary human hepatocytes (PHHs) and several human hepatoma cell lines (HepaRG, HuH-7, HepG2, and HepG2/C3A). Furthermore, genes associated with hepatotoxicity, drug-metabolizing enzymes, transporters, and nuclear receptors were extracted for more detailed comparisons. Our results showed that iPSC-Heps correlate more closely to PHHs than hepatoma cell lines, suggesting that iPSC-Heps had a relatively mature hepatic phenotype that more closely resembles that of adult hepatocytes. HepaRG was the sole exception but nonetheless suffers from lack of donor diversity and poor prediction of hepatotoxicity. The effects of sex differences and DMSO treatment on gene expression of the cellular models were also investigated. Overall, the results presented in the current study suggest that iPSC-Heps represent a reproducible source of human hepatocytes and a promising in vitro model for hepatotoxicity evaluation. Further studies are needed to develop a robust protocol for hepatocyte differentiation towards a more mature adult phenotype.

Abbreviations

ANOVA	Analysis of variance
cDNA	Complimentary deoxyribonucleic acid
cRNA	Complimentary ribonucleic acid
CYP	Cytochrome P450
DEG	Differentially expressed gene
DMEM	Dulbecco's Modified Eagle Medium
DMSO	Dimethyl sulfoxide
FC	Fold change
FDR	False discovery rate
HCA	Hierarchical clustering analysis
HEPES	4-(2-hydroxyethyl)-1-piperazineethanesulfonic acid
iPSC	Induced pluripotent stem cell
iPSC-Hep	Induced pluripotent stem cell-derived hepatocyte
IVT	In vitro transcription

X. Gao (✉) · Y. Liu (✉)
Division of Applied Regulatory Toxicology, Office of Applied Research and Safety Assessment, Center for Food Safety and Applied Nutrition, U.S. Food and Drug Administration, Laurel, MD 20708, USA
e-mail: xiugong.gao@fda.hhs.gov
e-mail: yitong.liu@fda.hhs.gov

MEM	Minimal essential medium
PCA	Principal component analysis
PHH	Primary human hepatocyte
RIN	RNA integrity number
RMA	Robust multi-array average (algorithm)
RPMI	Roswell Park Memorial Institute (medium)

Introduction

Unprecedented efforts are being made to develop predictive human in vitro models for liver toxicity and metabolism studies since animal testing suffers several limitations, including ethical issues, lack of human relevance, high cost, and long-time period needed to execute the study. Currently, primary human hepatocytes (PHHs), freshly isolated or stably cryopreserved, are considered the gold standard for drug metabolism and toxicity studies, as these cells express a comprehensive set of enzymes and transporters involved in hepatic drug clearance (Hewitt et al., 2007). However, several major drawbacks have hindered their widespread use: rapid decline of functionality under in vitro tissue culture environment (Richert et al., 2006), restricted availability, and enormous variability in the overall cell quality between different donors or preparations.

A number of hepatoma-derived cell lines such as HepG2 and HuH-7 have also been employed in hepatotoxicity assessment over the past decades. Although they have overcome some of the limitations of PHHs owing to their unlimited availability and phenotypic stability, these cell lines have their own shortcomings. Of most importance, they are limited in terms of drug-metabolizing functionality (Gerets et al. 2012), which renders them inadequate for metabolite toxicity testing. The creation of the HepaRG cell line represents a major improvement over previous cell models in terms of hepatocyte functionality, particularly in the activity of major CYP enzymes and the expression of nuclear receptors (Aninat et al. 2006). However, this cell line suffers low predictivity of hepatotoxicity (Gerets et al. 2012), probably due to its origin from a tumor background thus exhibiting reduced sensitivity to toxic insults.

The recent advent of hepatocytes derived from human induced pluripotent stem cells (iPSCs) represents an attractive alternative to PHHs and hepatoma cell lines as in vitro liver models (Si-Tayeb et al. 2010; Sullivan et al. 2010). First reported by Yamanaka and co-workers in 2006 from fibroblast using retroviral vectors (Takahashi and Yamanaka, 2006), iPSCs can now be generated from a variety of somatic source cells using diverse reprogramming techniques, either integrating or non-integrating, for the delivery of reprogramming factors (Raab et al. 2014; Singh et al. 2015), which makes it possible to generate iPSCs from virtually any donor. Subsequently, iPSCs can be differentiated into almost all somatic cell types, hence provide a well-defined source for deriving tissue-specific cell types, including hepatocytes, for use as in vitro models for toxicological studies as well as for disease modeling (Asgari et al. 2010; Suter-Dick et al. 2015). Although still in its infancy, iPSC-derived hepatocytes (iPSC-Heps) hold great promise with potential applications in pharmacology, toxicology, and tissue engineering. Compared to PHHs, iPSC-Heps are sustainable of function in long-term culture with unlimited and consistent supply; while comparing to hepatoma cell lines; iPSC-Heps do not originate from hepatomas and could be derived from diverse populations (Mann 2015). Nevertheless, the suitability of iPSC-Heps for drug metabolism and toxicity studies has yet to be established, particularly in terms of expression of drug-metabolizing enzymes and transporters as well as stable functionality over time in culture.

In the current study, we used a transcriptomic approach to characterize iPSC-Heps in comparison to PHHs and hepatoma-derived cell lines. First, global gene expression profiles of various in vitro cell models were compared. Secondly, gene expression related to hepatotoxicity, drug-metabolizing enzymes, transporters, and nuclear receptors were extracted for detailed analysis. Next, potential effect of sex differences among cell models was evaluated. Lastly, since dimethyl sulfoxide (DMSO) has been found to induce differentiation of stem cells and tumor-originated cell lines (Andersson et al. 2012; Jacob and Herschler 1986; Santos et al. 2003), the effects of DMSO treatment (1.0%) on gene expression were investigated in iPSC-Heps and hepatoma HuH-7 cells.

Materials and methods

Materials

Cell culture media and medium supplements (RPMI medium, DMEM medium, B27 supplement,

dexamethasone, gentamicin, and rat tail collagen type I) were all obtained from Thermo Fisher Scientific (Waltham, MA) except for oncostatin M, which was obtained from R&D Systems (Minneapolis, MN), and fetal bovine serum, which was purchased from Atlanta Biologicals (Lawrenceville, GA). DMSO was obtained from Sigma-Aldrich (St. Louis, MO).

Cell models and cell culture

iCell Hepatocytes 2.0 were purchased from Cellular Dynamics International (Madison, WI) together with the proprietary iCell Hepatocytes 2.0 Medium Supplement. According to the manufacturer, the cells were derived from an iPSC line generated from the fibroblasts of a young (0–18-years old) Caucasian female with no known disease phenotype, through ectopic expression of reprogramming factors (i.e., Oct4, Sox2, Nanog, Lin28) by retroviral transduction. iCell Hepatocytes 2.0 were differentiated from the iPSC line by directed differentiation, employing sequential addition of small molecules and growth factors. The proprietary process was monitored by marker expression characterization at the stages of endoderm formation, hepatoblasts specification, and terminal differentiation to hepatocytes. In the current experiment, iCell Hepatocytes 2.0 cells were cultured following the manufacture's protocols. Briefly, cells were thawed and seeded onto rat tail collagen type I coated surfaces (3×10^5 cells/cm^2) using Plating Medium composed of RPMI medium, B27 supplement, oncostatin M (20 μg/ml), dexamethasone (0.1 μM), gentamicin (25 μg/ml), and the Medium Supplement. Plating Medium was replenished daily for 4 days after seeding. On day 5, Plating Medium was replaced by Maintenance Medium, which was composed of RPMI medium, B27 supplement, dexamethasone (0.1 μM), gentamicin (25 μg/ml), and the Medium Supplement. Maintenance Medium was refreshed every 2 days. iCell hepatocytes were used for microarray studies under three conditions: cells post thawing (iHep), cells cultured for 2 weeks after seeding without treatment (iHepCtrl), and cells cultured for 2 weeks and treated with DMSO (1.0%) during the second week (iHepDMSO).

PHHs (from three male and three female donors, respectively) were obtained from Bioreclamation IVT (Baltimore, MD). Cells were thawed, washed, and used for microarray studies without any treatment. The demographics of the PHH donors are listed in Supplemental Table 1.

Human hepatoma HuH-7 cells were purchased from Health Science Research Resources Bank, Japan Health Sciences Foundation (Osaka, Japan). Cells were seeded onto rat tail collagen type I coated surfaces (6×10^4 cells/cm^2) and cultured in Dulbecco's Modified Eagle Medium (DMEM) with low glucose, pyruvate, GlutaMAX, MEM non-essential amino acids, and HEPES (10 mM), supplemented with fetal bovine serum (10%). No antibiotics were added to the medium. HuH-7 cells were used for microarray studies under four conditions: cells without treatment (HuH), cells treated with DMSO (1.0%) for one, two or 3 weeks (HuH1w, HuH2w, and HuH3w). DMSO treatment started after cell reached confluence, which was about 3 days after seeding.

HepG2 cells were a gift from National Center for Advancing Translational Sciences, National Institutes of Health (Bethesda, MD). HepG2/C3A cells were obtained from ATCC (Manassas, VA). HepaRG cells were purchased from Thermo Fisher Scientific. HepG2, HepG2/C3A, and HepaRG were thawed, washed, and used for microarray studies without any treatment.

RNA extraction and quality assurance

Cultured cells were harvested and stored at −80 °C before RNA extraction. Cells were lysed in RLT buffer (Qiagen, Valencia, CA) and homogenized using QIAshredder (Qiagen). Cell lysates were extracted for total RNA using EZ1 RNA Cell Mini Kit (Qiagen) on EZ1 Advanced XL automated RNA purification instrument (Qiagen) following the manufacture's protocol, including an on-column DNase digestion. Total RNA concentration and purity were subsequently measured using NanoDrop 2000 UV-Vis spectrophotometer (NanoDrop Products, Wilmington, DE). RNA integrity was further analyzed by Agilent 2100 Bioanalyzer (Agilent, Santa Clara, CA) using the RNA 6000 Nano Reagent Kit from the same manufacturer.

Microarray experiment

All reagents and instruments used for the microarray experiment were obtained from Affymetrix (Santa Clara, CA). Total RNA from different cell samples was processed for gene expression profiling on GeneChip PrimeView Human Gene Expression Arrays using GeneChip 3″ IVT PLUS Reagent Kit following the manufacture's protocol.

Briefly, 100 μg total RNA was used to generate single-stranded complementary DNA (cDNA) using reverse transcriptase and a T7-linked oligo (dT) primer. Single-stranded cDNA was then converted to double-stranded cDNA using DNA polymerase and RNase H. The second strand of the double-stranded cDNA served as a template for the subsequent in vitro transcription (IVT) to synthesize the complementary RNA (cRNA) with biotinylated UTP and CTP using T7 RNA polymerase. The labeled cRNA was then purified and measured for concentration.

The purified cRNA (12 μg) was fragmented by divalent cations (Mg^{2+}) at an elevated temperature (94 °C). Fragmented and labeled cRNA was hybridized to the GeneChip PrimeView Human Gene Expression Arrays at 45 °C for 16 h in the GeneChip Hybridization Oven 645. After hybridization, the array chips were stained and washed using the GeneChip Fluidics Station 450. Finally, the chips were scanned using GeneChip Scanner 3000 7G. The scanned image (.DAT) files were preprocessed using Affymetrix GeneChip Command Console software 4.0 to produce cell intensity (.CEL) files. Prior to data analysis, all arrays were assessed for data quality using Affymetrix Expression Console software 1.3.

Data analysis

The values of individual probes belonging to one probe set in CEL files were summarized using the robust multi-array average (RMA) algorithm (Irizarry et al. 2003) embedded in the Affymetrix Expression Console software 1.3 which comprises of convolution background correction, quantile normalization, and median polish summarization. Principal component analysis (PCA) and hierarchical clustering analysis (HCA) were conducted using ArrayTrack, a software package for analyzing and interpreting microarray gene expression data, developed by the National Center for Toxicological Research at the U.S. Food and Drug Administration (Tong et al. 2003).

The distance between two samples in the 15-dimensional PCA space was calculated from the differences between the scores of the 15 components (PC_1, PC_2, …, PC_{15}) of the two data points using the following formula: $d = (\Delta PC_1^2 + \Delta PC_2^2 + \ldots + \Delta PC_{15}^2)^{\frac{1}{2}}$. The center for multiple samples in the PCA space was calculated as the mean of the data points for each of the 15 component scores, i.e., the center has the component scores as ($\overline{PC1}$, $\overline{PC2}$, …, $\overline{PC15}$).

Statistical analysis for the selection of differentially expressed genes (DEGs) between two experimental groups was conducted using Affymetrix Transcriptome Analysis Console software 2.0, based on one-way analysis of variance (ANOVA) and Welch t test. For each comparison, the fold change (FC) of every annotated gene, together with their ANOVA p value or false discovery rate (FDR), was used for the selection of DEGs with cutoff values described in the text.

Results

The in vitro cell models employed in the current study include one line of iPSC-Heps, PHHs from six individual donors, and four human hepatoma cell lines (HepaRG, HuH-7, HepG2, and HepG2/C3A). To evaluate potential sex differences among the cell models, cell lines of both male and female origins were included. Cell models of male origin included PHHs from three male donors, HuH-7, HepG2, and HepG2/C3A; female origin included PHHs from three female donors, iPSC-Heps, and HepaRG. To assess the effects of DMSO treatment, iPSC-Heps and HuH-7 cells were treated with 1.0% DMSO for different periods and were compared to untreated controls.

Within 24 h after plating, iHeps formed an adherent monolayer and displayed a typical cobblestone morphology closely resembled that of PHHs, with high cytoplasmic-to-nuclear ratio and multiple and prominent nucleoli. Binucleated cells and formation of bile canaliculi between adjacent cells became evident after 3 days in culture (Fig. 1). The cells remained viable and adherent in culture throughout the experiment (14 days). DMSO treatment had no effect on the morphology of iHeps (data not shown). In addition, no significant cell death was observed during DMSO treatments. All RNA samples passed the RNA quality analysis with RNA integrity number (RIN) ≥ 8.0. Before data analysis, all arrays referred to in this study were assessed for data quality with all quality assessment metrics (including spike-in controls during target preparation and hybridization) within default boundaries.

Global gene expression analysis

The global gene expression data were first analyzed by PCA to compare the different cellular models. PCA provides a means to reduce high-dimensional gene
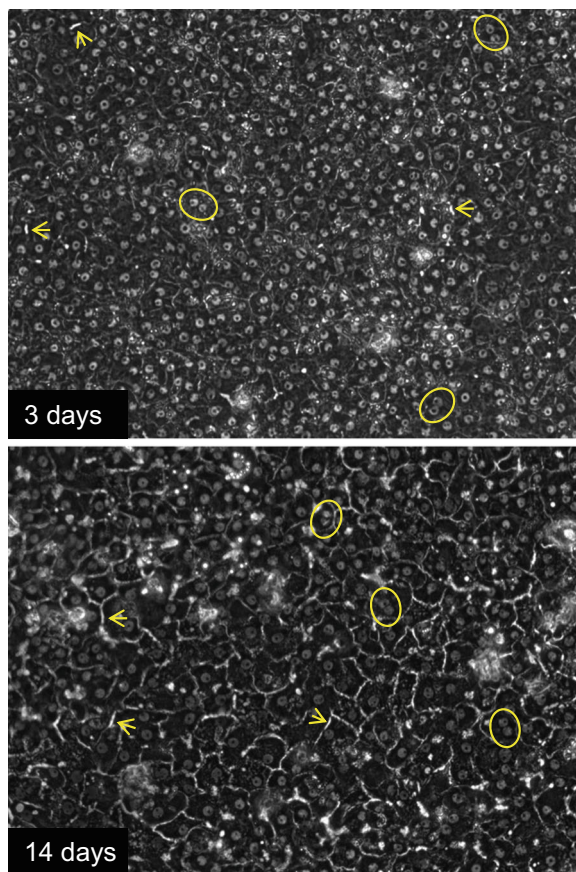
Fig. 1 Morphology of induced pluripotent stem cell (iPSC)-derived hepatocytes (iPSC-Heps) after 3 and 14 days in culture. Representative phase-contrast light microscopy images are shown with magnification at ×100. The *arrows* denote bile canaliculi formation and the *circles* indicate binucleated cells

expression data into few principal components (Ringner 2008). Gene expression profiles are considered to be similar when samples fall in close proximity to one another in PCA plot. As shown in Fig. 2a, overall the samples were clustered into three major groups corresponding to the three major cellular models: iPSC-Heps, PHHs, and hepatoma cell lines. An exception was HepaRG, which did not cluster with other hepatoma cell lines but fell in between the other hepatoma cell lines and PHHs along the axis of the first principal component (PC1). The three samples of iPSC-Heps also fell in between the hepatoma cell lines and PHHs along PC1, but shifted away from HepaRG along PC3. Within the PHH cluster, samples of different sex were mixed with no discrete boundaries, suggesting sex played little effect on global gene expression level. It was interesting to note that the two hepatoma cell lines HepG2 and

HepG2/C3A almost fell onto each other. This is not surprising when considering that HepG2/C3A is a clonal derivative of HepG2 (Flynn and Ferguson 2008). It was also noted that treatment with DMSO had some major impact on HuH-7 cells, although treatment duration made limited differences.

The global gene expression data were further analyzed by HCA. Using Ward's minimum variance method (Ward 1963), HCA yielded a hierarchy of clusters presented in the form of a dendrogram based on the similarities between samples. As shown in Fig. 2b, the cell models were grouped into two major clusters: one consists of the PHHs, the other of all other cell models. Consistent with the PCA result, no sex differences were observed in the PHH cluster. Within the other cluster, iPSC-Heps and HepaRG cells grouped closely, while HepG2, HepG2/C3A, and HuH-7 clustered together. Although iPSC-Heps and HepaRG cells were from female donors, and HepG2, HepG2/C3A, and HuH-7 cells were from male donors, the data are insufficient to attribute the grouping to sex differences.

The distances of each of the cell models to the center of the PHH cluster in the PCA space were calculated and were used to rank these models in terms of their similarity to the PHHs. The result (Fig. 2c) showed that iPSC-Heps and HepaRG cells more closely resembled PHHs than the rest of the cell models on global gene expression. Detailed gene expression analysis was subsequently conducted on genes related to the unique functions of the liver: hepatotoxicity, drug-metabolizing enzymes, transporters, and nuclear receptors.

Hepatotoxicity related genes

The cell models were further compared using a list of genes related to cholestasis, steatosis, phospholipidosis, non-genotoxic hepatocarcinogenicity, necrosis, and general hepatotoxicity (Supplemental Table 2), which was adapted from a previously published study (Koturbash et al. 2011). The PCA plot using this gene list (Fig. 3a) was very similar to that of whole genome analysis (Fig. 2a) in terms of sample clustering, except that untreated HuH-7 moved farther away from its DMSO treated siblings. This is consistent with HCA, where cell models were grouped into two major clusters (Fig. 3b): one consists of PHHs, the other of all other cell models. Within the latter cluster, it could be seen that HuH-7 formed a subcluster with HepG2 and HepG2/C3A, while DMSO-treated HuH-7 cells formed
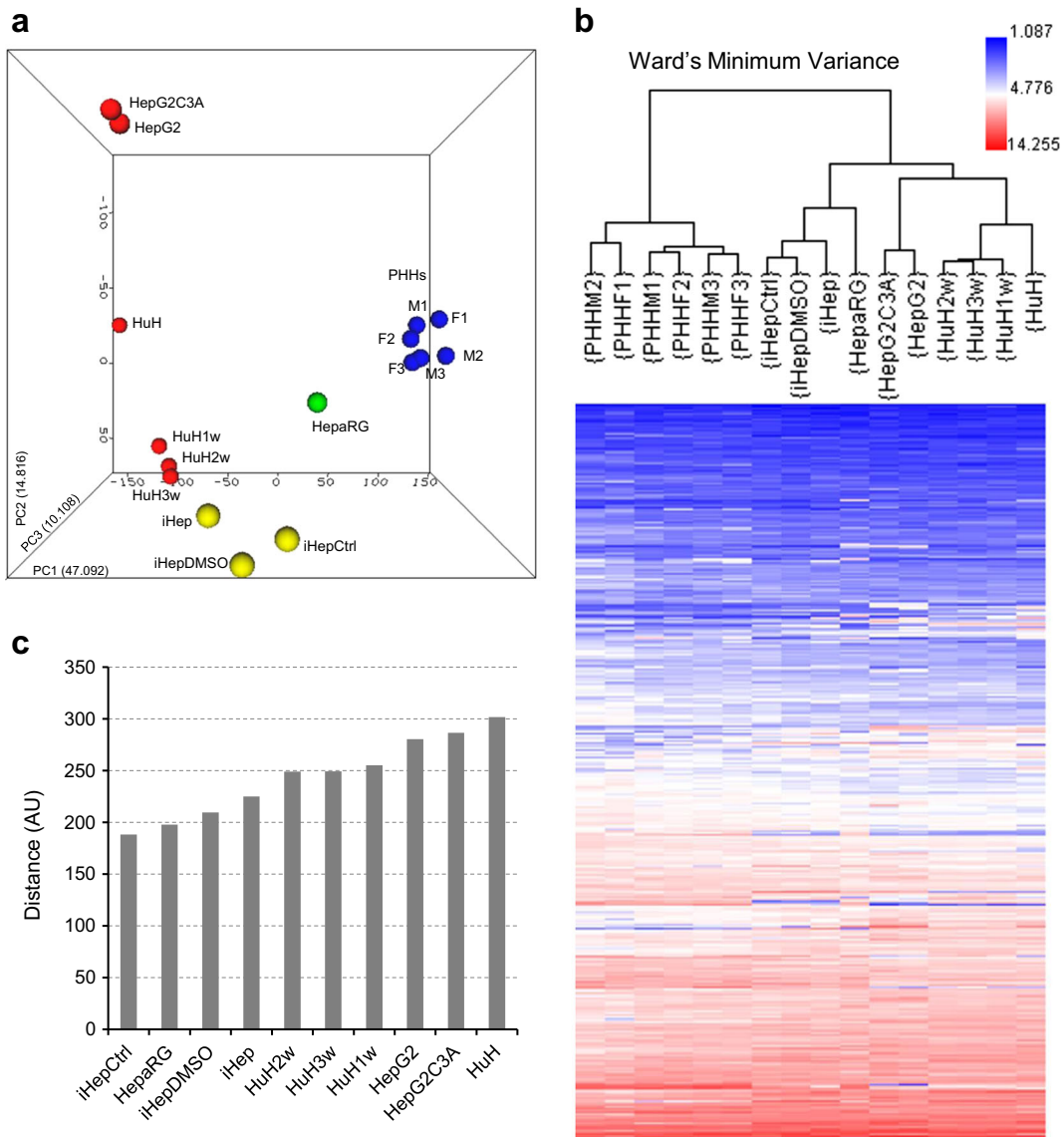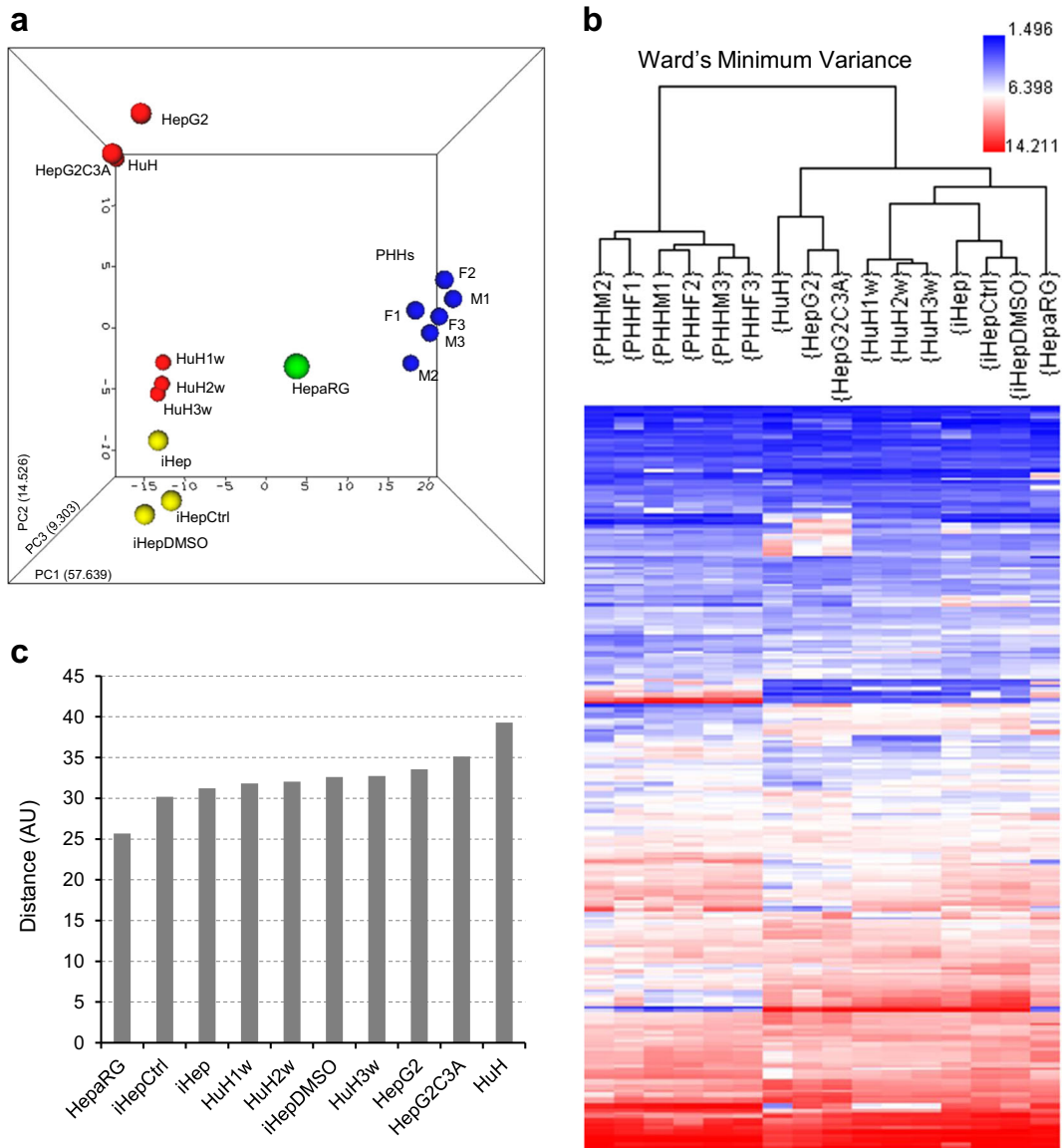
Fig. 2 Comparison of different cell models using global gene expression data. **a** Principal component analysis (PCA). The three axes PC1, PC2, and PC3 represent the first three principal components identified by the analysis. **b** Hierarchical clustering analysis (HCA). The clustering was performed through Ward's minimum variance linkage on normalized expression data which are in log2 scale and color coded as shown in the scheme at the top right corner. The *dendrogram* on top of the image shows clustering of the samples. **c** *Bar graph* showing distances of each of the cell models to the center of the PHHs in the PCA space. *PHHs* primary human hepatocytes, including three females (F1, F2, F3) and three males (M1, M2, M3), *iHep* iPSC-Heps post thawing, *iHepCtrl* iPSC-Heps cultured for 2 weeks, *iHepDMSO* iPSC-Heps treated with DMSO for 1 week, *HuH* untreated HuH-7 cells; *HuH1w*, *HuH2w*, and *HuH3w* HuH-7 cells treated with DMSO for 1, 2, and 3 weeks, respectively

another subcluster with iPSC-Heps and HepaRG. Distances of the cell models to the center of the PHH cluster in the PCA space (Fig. 3c) showed that HepaRG was the closest to PHHs, followed by iPSC-Heps, DMSO-treated HuH-7 cells, HepG2, and HepG2/C3A. HuH-7 was much further way from the PHHs than the other cell models.

Liver drug-metabolizing enzymes, transporters, and nuclear receptors

Another list of genes (Supplemental Table 3) related to drug-metabolizing enzymes (phases I and II), transporters, and nuclear receptors (Lu et al. 2015) were selected to compare the cell models. A major difference in the PCA
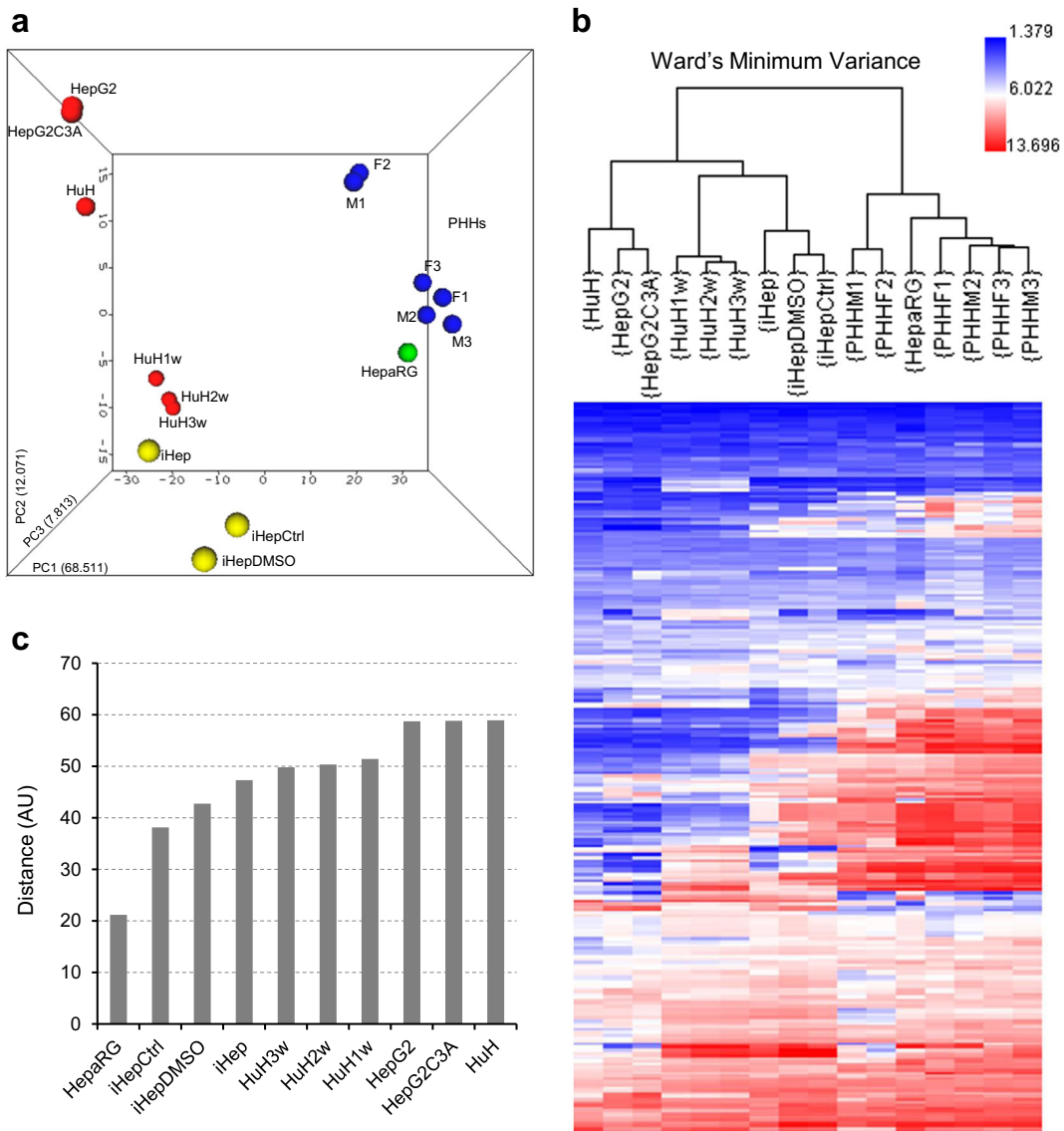
Fig. 3 Comparison of different cell models using hepatotoxicity related genes. The list of genes is provided in Supplemental Table 2. **a** Principal component analysis (PCA). The three axes PC1, PC2, and PC3 represent the first three principal components identified by the analysis. **b** Hierarchical clustering analysis (HCA). The clustering was performed through Ward's minimum variance linkage on normalized expression data which are in log2 scale and color coded as shown in the scheme at the top right corner. The *dendrogram* on top of the image shows clustering of the samples. **c** *Bar graph* showing distances of each of the cell models to the center of the PHHs in the PCA space. *PHHs* primary human hepatocytes, including three females (F1, F2, F3) and three males (M1, M2, M3), *iHep* iPSC-Heps post thawing, *iHepCtrl* iPSC-Heps cultured for 2 weeks, *iHepDMSO* iPSC-Heps treated with DMSO for 1 week, *HuH* untreated HuH-7 cells; *HuH1w*, *HuH2w*, and *HuH3w* HuH-7 cells treated with DMSO for 1, 2, and 3 weeks, respectively

plot using this gene list (Fig. 4a) from the previous analyses using the whole genome (Fig. 2a) or genes related to hepatotoxicity (Fig. 3a) was that in the current analysis the six PHHs were not clustered close together, with two PHHs (F2 and M1) falling far away from the other four (F1, F3, M2, M3), suggesting differences in the expression of

this subset of genes between the PHH samples. Interestingly, HepaRG, a highly metabolically competent hepatoma cell line, was closer to the larger PHH subcluster (M2, M3, F1, F3) than M1 and F2. This was also reflected in the HCA, where HepaRG grouped with PHHs in one of the two major clusters and split the PHHs into two subclusters (Fig. 4b).

Fig. 4 Comparison of different cell models using liver metabolism, transporter, and nuclear receptor related genes. The list of genes is provided in Supplemental Table 3. **a** Principal component analysis (PCA). The three axes PC1, PC2, and PC3 represent the first three principal components identified by the analysis. **b** Hierarchical clustering analysis (HCA). The clustering was performed through Ward's minimum variance linkage on normalized expression data which are in log2 scale and color coded as shown in the scheme at the top right corner. The *dendrogram* on top of the

image shows clustering of the samples. **c** *Bar graph* showing distances of each of the cell models to the center of the PHHs in the PCA space. *PHHs* primary human hepatocytes, including three females (F1, F2, F3) and three males (M1, M2, M3), *iHep* iPSC-Heps post thawing, *iHepCtrl* iPSC-Heps cultured for 2 weeks, *iHepDMSO* iPSC-Heps treated with DMSO for 1 week, *HuH* untreated HuH-7 cells; *HuH1w*, *HuH2w*, and *HuH3w* HuH-7 cells treated with DMSO for 1, 2, and 3 weeks, respectively

All other cell models grouped together into the other major cluster. Distances of the cell models to the center of the PHH cluster in the PCA space (Fig. 4c) showed the following ranking in terms of similarity with PHHs: HepaRG, iPSC-Heps, DMSO-treated HuH-7 cells, HepG2, HepG2/C3A, and HuH-7 cells. HepaRG was much closer than the rest of

the cell models to the PHHs, while HepG2, HepG2/C3A, and HuH-7 were on par with one another.

Relative gene expression of major phase I drug-metabolizing cytochrome P450 (CYP) enzymes and functionally relevant transporters were compared across the cell models. As shown in Fig. 5a, there were

a

	HepG2	HepG2 C3A	HuH	HuH2w	iHep	iHep Ctrl	iHep DMSO	HepaRG	PHH Ave
CYP1A1	4.9	4.3	5.1	4.4	5.2	5.5	4.8	4.5	5.4
CYP1A2	5.6	5.3	5.3	5.4	5.6	6.0	5.5	5.9	8.6
CYP2B6	3.6	3.7	3.2	3.5	3.4	3.7	3.3	7.3	7.0
CYP2C19	2.5	2.4	2.4	3.2	4.4	5.1	3.3	6.6	6.7
CYP2C8	2.8	2.8	2.8	2.8	4.9	4.1	4.0	10.4	11.1
CYP2C9	2.5	2.6	3.3	3.5	5.6	6.8	5.8	10.0	9.2
CYP2D6	5.5	6.0	5.1	5.4	6.3	6.5	5.8	5.3	11.0
CYP2E1	2.6	2.2	2.4	2.7	2.9	3.5	3.0	10.2	12.1
CYP3A4	3.2	3.3	3.2	4.5	4.6	8.6	7.4	12.2	10.1
CYP3A5	5.4	4.9	3.7	6.2	6.5	9.2	9.5	10.7	9.3
CYP3A7	6.0	7.3	6.6	12.1	11.9	13.4	13.4	7.7	8.5

1.5　　　　　　　　7.5　　　　　　　　13.5

b

	HepG2	HepG2 C3A	HuH	HuH2w	iHep	iHep Ctrl	iHep DMSO	HepaRG	PHH Ave
ABCB1	5.8	6.3	5.2	5.3	3.3	3.8	3.6	6.6	5.5
ABCB11	2.2	2.2	2.5	3.1	4.3	6.7	6.5	3.6	6.0
ABCB4	5.7	5.6	3.8	6.4	4.2	5.9	5.1	8.4	8.6
ABCC2	9.4	9.6	7.0	7.9	8.2	8.8	8.6	9.8	8.5
ABCC3	6.9	7.1	4.5	4.2	7.4	8.4	7.9	8.6	8.4
ABCC4	4.1	3.4	4.6	3.3	4.0	3.8	4.3	3.7	3.0
ABCG2	4.8	4.2	4.7	3.7	4.3	3.9	4.2	4.5	4.6
SLC15A1	2.6	2.7	2.7	3.5	3.7	5.4	5.5	3.1	4.0
SLC15A2	3.4	3.6	3.7	4.4	4.1	3.8	3.6	3.7	3.9
SLC22A1	3.8	4.0	3.8	5.1	5.2	8.7	7.7	11.2	11.5
SLC22A2	3.0	3.0	2.9	3.0	3.1	3.3	3.1	3.1	3.4
SLC22A6	3.7	3.7	3.4	3.5	3.7	3.7	3.6	3.5	4.1
SLC22A8	4.4	4.5	4.3	4.5	4.6	4.8	4.6	4.8	5.1
SLC47A1	6.2	6.7	6.1	6.7	6.0	7.0	7.1	6.7	6.5
SLC47A2	4.2	4.0	3.8	4.4	4.6	4.8	4.4	7.2	4.9
SLCO1A2	1.9	1.9	2.7	4.3	2.1	2.2	2.1	2.1	2.5
SLCO1B1	3.8	3.8	4.0	3.9	5.4	7.8	5.9	8.1	9.4
SLCO1B3	2.8	2.4	4.5	2.9	2.4	1.9	2.0	3.5	8.0
SLCO2B1	5.2	5.9	5.1	7.2	7.6	8.0	8.1	7.4	7.5

Fig. 5 Relative gene expression of major cytochromes P450 enzymes (**a**) and functional transporters (**b**). Gene expression values were the average of the probesets for each enzyme or transporter, which are in log2 scale and color coded as shown in the scheme located in the middle of the figure. The values for primary human hepatocytes (PHH Ave) were the average of six individuals, including three female and three male donors. *iHep* iPSC-Heps post thawing, *iHepCtrl* iPSC-Heps cultured for 2 weeks, *iHepDMSO* iPSC-Heps treated with DMSO for 1 week, *HuH* untreated HuH-7 cells; *HuH2w* HuH-7 cells treated with DMSO for 2 weeks. HuH1w and HuH3w had similar values with those of HuH2w and therefore are not shown

enormous differences in the expression of these CYP enzymes among the cell models. HepaRG most closely resembled PHHs, followed by iPSC-Heps, and lastly the remaining cell lines. Notably, CYP3A7, a fetal phenotype in the CYP3A family, was highly expressed in both iPSC-Heps and DMSO-treated HuH-7 cells. However, in PHHs and HepaRG cells, adult phenotypes of CYP3A (CYP3A4 and CYP3A5) dominate. Additionally, all the cell models except PHHs exhibited low expression of CYP1A2 and CYP2D6, which is consistent with published reports (Choi et al. 2009; Gerets et al. 2012; Hart et al. 2010).

Expression of functionally relevant transporters (Fig. 5b) generally followed the same pattern as the CYP enzymes, with HepaRG most closely resembling PHHs, followed by iPSC-Heps and then the remaining cell lines. Exceptions were HepG2 and HepG2/C3A, of which the expression of several transporters, including ABCB1, ABCB4, ABCC2, ABCC3, and SLC47A1, was comparable to, or even higher than, that in iPSC-Heps. It was interesting to note that ABCB11, more commonly referred to as BSEP (bile salt export pump), which is an efflux transporter that plays important roles in the secretion of bile salts from the liver into the bile canaliculi for export into the gut (Cheng et al. 2007), had the highest expression in iPSC-Heps than all other cell models. On the other hand, ABCG2, or BCRP (breast cancer resistance protein), another efflux transporter that plays an important role in drug disposition and distribution similar to P-glycoproteins (Maliepaard et al. 2001), had very similar expressions across all cell models.

Differential gene expression between different sex groups in primary human hepatocytes

Gene expression differences were analyzed between the two sex groups of the PHHs. Out of the total 49,372 genes present on the array, 165 genes were found differentially expressed (|FC| >2, $p < 0.05$), with 97 genes upregulated and 68 genes downregulated (Supplemental Table 4). However, the majority of these genes had a very high FDR value (>0.9), suggesting they are false positives. Only three genes had a FDR < 0.5, all of which were located in either the X or the Y chromosome (Fig. 6). XIST is a non-protein coding, X inactive specific transcript, which was expressed >270-fold in female PHHs than in their male counterparts. EIF1AY is a eukaryotic translation initiation factor, and RPS4Y1 a ribosomal protein S4, both were Y-linked and were expressed 38-fold and 40-fold higher, respectively, in the male PHHs than in the females. Therefore, the
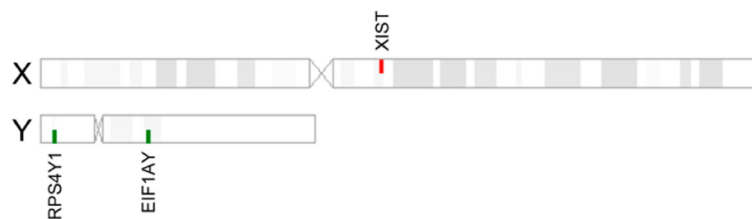
differences between the two sex groups of PHHs were confined to sex-related genes only.

Effect of DMSO treatment in HuH-7 cells and in iPSC-derived hepatocytes

In the current study, DMSO treatment demonstrated dramatic effects on gene expression profiles in HuH-7 cells. Without DMSO treatment, HuH-7 cells clustered with HepG2 and HepG2/C3A cells, which were least similar to PHHs compared with other models. However, after DMSO treatment for 1, 2, or 3 weeks, HuH-7 cells fell much closer to PHHs on the PCA plot (Figs. 2c, 3c, 4c). While still clustered together with untreated HuH-7, HepG2 and HepG2/C3A cells on the global genome level (Fig. 2b), DMSO-treated HuH-7 cells clustered with iPSC-Heps both on hepatotoxicity-related genes (Fig. 3b) and on drug-metabolizing enzymes, transporters, and nuclear receptors (Fig. 4b). DMSO treatment induced gene expression of all CYP3A isoforms including CYP3A4, 3A5, and 3A7 in HuH-7 cells (Fig. 5a). On the other hand, DMSO treatment had limited effects in iPSC-Heps (Figs. 2–5). In addition, DMSO treatment duration (1–3 weeks) had minimal effects in HuH-7 cells, either on the global gene expression level (Fig 2c), or for the expression of hepatotoxicity-related genes (Fig. 3c), drug-metabolizing enzymes, transporters, and nuclear receptors (Fig. 4c).

Discussions

Since the first reports on the generation of hepatocytes from iPSCs (Si-Tayeb et al. 2010; Sullivan et al. 2010), many proof-of-concept studies have already shown utility of these cells in drug screening and toxicity testing, liver disease modeling, and cell-based therapies as well (Schwartz et al. 2014; Sun et al. 2015). However, the suitability of iPSC-Heps in drug metabolism and

Fig. 6 Chromosome maps showing the location of the three genes differentially expressed between the two sex groups of primary human hepatocytes on the X and Y chromosomes. Upregulated genes (female vs. male) are plotted on the top of a chromosome in *red*. Downregulated genes are plotted at the bottom of a chromosome in *green*

toxicity testing has not been well established. In particular, a systematic study is lacking comparing iPSC-Heps with other liver cell models currently in use. In the present study, we used a transcriptomic approach to compare iPSC-Heps with PHHs and hepatoma-derived cell lines, first on the whole genome level, then focused on hepatotoxicity related genes, drug-metabolizing enzymes, transporters, and nuclear receptors. To the best of our knowledge, no similar study has been reported previously.

Our results showed that on the whole genome level, iPSC-Heps correlated more closely to PHHs than the hepatoma cell lines except for HepaRG, which was on par with iPSC-Heps. This suggests that iPSC-Heps had a relatively mature hepatic phenotype that more closely resembles that of adult hepatocytes than most of the hepatoma cell lines. More detailed analysis on hepatotoxicity related genes, and on drug-metabolizing enzymes, transporters, and nuclear receptors corroborated these findings. These analyses showed that iPSC-Heps, although behind HepaRG, outperformed all other hepatoma cell lines (HepG2, HepG2/C3A, and HuH-7) (Figs. 2–4). Taken together, these results suggest that iPSC-Heps offer a better in vitro model for toxicology studies than most hepatoma cell lines.

Several studies have reported successful detection of hepatotoxicity using iPSC-Heps. In one study, it was shown that hepatotoxic compounds acetaminophen, troglitazone, and nefazodone exhibited similar cytotoxicity in iPSC-Heps and in PHHs after a 24-h treatment (Lu et al. 2015). In another study, iPSC-Heps co-cultured with murine embryonic fibroblasts successfully identified 24 out of 37 hepatotoxic drugs with comparable accuracy of PHHs co-cultured with murine embryonic fibroblasts (Ware et al. 2015). Several other reports draw similar conclusion that iPSC-Heps are promising as an in vitro model for hepatotoxicity evaluation (Mann 2015; Medine et al. 2013; Sirenko et al. 2014; Takayama et al. 2013), especially for extended treatment periods (Holmgren et al. 2014). On the other hand, hepatoma derived cell lines, such as HepG2 and HepaRG, lacked sensitivity in predicting hepatotoxicity due to their origins from a tumor background (Gerets et al. 2012; Liu et al. 2015).

A number of hepatoma-derived cell models have been used in the past decades in various pharmacology and toxicology studies. However, limited literature is available for a global characteristic comparison of these models in order to facilitate the selection of cell lines for specific applications, such as hepatotoxicity or drug metabolism. The current study filled this gap by characterizing these cell models on the gene expression level in comparison to PHHs. HepG2 cells were derived from a Caucasian male with primary liver carcinoma (Aden et al. 1979). These cells are highly differentiated and displayed many of the genotypic features of normal liver cells (Sassa et al. 1987). Their main limitation is low metabolic capacity compared with PHHs (Xu et al. 2004), which make them less suited for metabolite toxicity testing albeit appropriate for testing the toxicity of the parent molecules. HepG2/C3A is a clonal derivative of HepG2 possessing several desirable properties, including strong contact inhibition of growth and high albumin production (Flynn and Ferguson 2008). Our results showed that HepG2 and HepG2/C3A are very similar both in global gene expression pattern, and in the expression of specific genes related to hepatotoxicity, and drug-metabolizing enzymes, transporters, and nuclear receptors. Expression of CYP enzymes was very low in both cell types (Fig. 5a). Another unrelated cell line, HuH-7, which was derived from a Japanese male with well-differentiated hepatocellular carcinoma (Nakabayashi et al. 1982), clustered with HepG2 and HepG2/C3A in all the analyses, suggesting their overall similarity.

An exception to the general inferiority of the hepatoma cell lines was HepaRG. Derived from a female patient with chronic hepatitis C infection and hepatocarcinoma, HepaRG cells are composed of both hepatocyte-like and biliary-like epithelial cells (Gripon et al. 2002). HepaRG cells have been highlighted for their high and inducible drug-metabolizing enzyme activities, which are comparable to PHHs (Andersson et al. 2012). Our results were consistent with previous studies. Ranked similarly with iPSC-Heps in global gene expression and slightly better in the expression of hepatotoxicity related genes, HepaRG cells outperformed iPSC-Heps in the expression of drug-metabolizing enzymes, transporters, and nuclear receptors, to a level on par with PHHs. Most CYP enzymes had similar expression levels to PHHS (Fig. 5a). Notably, CYP3A4, one of the most important CYP for drug metabolism, was expressed in HepaRG cells >4-fold higher than in PHHs. It was also interesting to note that CYP2D6 was >30-fold lower expressed in HepaRG cells in comparison to PHHs. This was not surprising as the patient from whom HepaRG cells were derived was a poor CYP2D6 metabolizer (Guillouzo et al.

2007). The high metabolic capacity of the HepaRG cells may qualify them as a useful tool for metabolism studies. However, it has to be noted that the high metabolic profile of HepaRG cells does not correlate with their predictivity of hepatotoxicity; the detection of hepatotoxic compounds in these cells was not remarkably better than in HepG2 cells (Gerets et al. 2012).

DMSO has been used to induce cell differentiation of hepatoma cells, including HepaRG (Andersson et al. 2012) and HuH-7 (Choi et al. 2009), as well as to maintain differentiated functions in long-term cultures of adult hepatocytes (Isom et al. 1985), and to enhance in vitro maturation of fetal liver cells (Sakai et al. 2002). The mechanism of action of DMSO is still poorly understood and can be diversed. Previously, DMSO has been shown to inhibit c-myc expression (Darling et al. 1989), arrest cell cycle progression thus affecting cell proliferation (Srinivas et al. 1991), and lead to the collapse of mitochondrial membrane potential resulting in apoptosis (Liu et al. 2001). Two very recent studies found that DMSO improves hepatic differentiation and maturation through downregulation of pluripotency genes (Czysz et al. 2015) and epigenetic modification (Cipriano et al. 2016). The current study showed that HuH-7 cells improved dramatically after DMSO treatment, which is in line with previous reports (Choi et al. 2009; Liu et al. 2015). HuH-7 cells have been shown to be a sensitive model for screening certain hepatotoxicants and CYP3A4 inhibitors after DMSO treatment (Liu et al. 2015). In contrast, DMSO had limited effects in iPSC-Heps. In fact, most of the CYP enzymes slightly decreased expression in iPSC-Heps upon DMSO treatment. The difference in the response to DMSO treatment between HuH-7 cells and iPSC-Heps is unclear. It is possible that different differentiation mechanisms exist between hepatoma cell lines and iPSC-derived hepatocytes, and further studies are needed to clarify. Functional maturation of iPSC-derived hepatocytes is an active area of research at present. It has been shown that presentation of cell-cell interactions through co-culture with other cells (Berger et al. 2015), presence of 3-dimensional (3D) scaffold during differentiation (Gieseck et al. 2014; Wang et al. 2016), or the combination of these two methods, namely, 3D co-culture (Nagamoto et al. 2012), can improve the differentiation and maturation of iPSC-derived hepatocytes.

iPSC-Heps cultured for 2 weeks after seeding showed some degree of improvement compared to cells post thawing (Figs. 2–5), e.g., CYP3A4 increased

expression by 16-fold (Fig. 5a), suggesting there is still room for further maturation of the iPSC-Heps. It is generally held that the current differentiation processes yield a cell population that is of a mixed phenotype: cells expressing adult liver genes (e.g., albumin, CYP3A4) and those expressing fetal liver genes (e.g., alpha-fetoprotein, CYP3A7) (Mann 2015). Therefore, more efforts are needed to improve the current differentiation protocol aiming at obtaining functional liver cells resembling PHHs.

Potential sex differences among the cell models were briefly evaluated in the current study. No impact of sex differences was observed in the PHHs in all the analyses (Figs. 2–5). DEGs between the two sex groups of PHHs were confined to sex-related genes only (Fig. 6). In contrast, in global gene expression analysis, it was noticed that within one of the two major clusters, iPSC hepatocytes and HepaRG cells, all of female origins, grouped into one subcluster, while HepG2, HepG2/C3A, and HuH-7, all of male origins, formed another subcluster, suggesting some differences between the two groups of cell models. It is unclear whether this difference is due to sex, or to the cell models per se. Since sex difference has been highlighted recently in toxicological studies (Kennedy 2016), a more systematic study on this topic is warranted.

It has to be pointed out that the current study has limitations. Primarily, due to the explorative nature of the study and the large number of cellular models involved, no replicates were included except for the PHHs, where triplicates were employed for each sex. Therefore, many of the statements made here do not have statistical support. In addition, to better qualify the iPSC-Heps for toxicity testing and drug metabolism studies, functional studies should be carried out in comparison to PHHs, such as cytotoxicity experiment using known hepatotoxic or nonhepatotoxic compounds, and CYP induction experiment using typical inducers such as beta-naphthoflavone, phenobarbital, and rifampicin (Berger et al. 2015; Lu et al. 2015). Nonetheless, collectively, the data presented here clearly show that iPSC-Heps correlated more closely to PHHs and may provide a better in vitro model for studying hepatotoxicity than most hepatoma cell lines except for HepaRG, which manifested a higher drug-metabolizing functionality than the iPSC-Heps. However, HepaRG is limited to a single genotype and thus not

representative of a broad patient population in toxicity studies. In contrast, iPSC-Heps could be generated from donors exhibiting a wide range of drug sensitivities and metabolizing backgrounds, and form a panel that is representative of a diverse population and therefore instrumental for predictive toxicity evaluation.

In summary, the results in the current study indicate that iPSC-Heps resembled PHHs more closely than most of the hepatoma cell lines in global gene expression patterns and in the expression of genes related to hepatotoxicity, drug-metabolizing enzymes, transporters, and nuclear receptors. Since iPSC-Heps afford donor diversity, unlimited long-term supply, along with stability and consistency in functionality, they represent a vast improvement over PHHs and tumor cell lines, and open up new possibilities for toxicology studies, drug discovery, and regenerative medicine.

Compliance with ethical standards

Conflict of interest statement The authors declare that they have no conflict of interest.

References

Aden DP, Fogel A, Plotkin S, Damjanov I, Knowles BB. Controlled synthesis of HBsAg in a differentiated human liver carcinoma-derived cell line. Nature. 1979;282:615–6.

Andersson TB, Kanebratt KP, Kenna JG. The HepaRG cell line: a unique in vitro tool for understanding drug metabolism and toxicology in human. Expert Opin Drug Metab Toxicol. 2012;8:909–20.

Aninat C, Piton A, Glaise D, Le Charpentier T, Langouet S, Morel F, Guguen-Guillouzo C, Guillouzo A. Expression of cytochromes P450, conjugating enzymes and nuclear receptors in human hepatoma HepaRG cells. Drug metabolism and disposition: the biological fate of chemicals. 2006;34:75–83.

Asgari S, Pournasr B, Salekdeh GH, Ghodsizadeh A, Ott M, Baharvand H. Induced pluripotent stem cells: a new era for hepatology. J Hepatol. 2010;53:738–51.

Berger DR, Ware BR, Davidson MD, Allsup SR, Khetani SR. Enhancing the functional maturity of induced pluripotent stem cell-derived human hepatocytes by controlled presentation of cell-cell interactions in vitro. Hepatology (Baltimore, Md). 2015;61:1370–81.

Cheng X, Buckley D, Klaassen CD. Regulation of hepatic bile acid transporters Ntcp and Bsep expression. Biochem Pharmacol. 2007;74:1665–76.

Choi S, Sainz Jr B, Corcoran P, Uprichard S, Jeong H. Characterization of increased drug metabolism activity in dimethyl sulfoxide (DMSO)-treated Huh7 hepatoma cells. Xenobiotica. 2009;39:205–17.

Cipriano, M., Correia, J.C., Camoes, S.P., Oliveira, N.G., Cruz, P., Cruz, H., Castro, M., Ruas, J.L., Santos, J.M., and Miranda, J.P. (2016). The role of epigenetic modifiers in extended cultures of functional hepatocyte-like cells derived from human neonatal mesenchymal stem cells. Archives of toxicology.

Czysz K, Minger S, Thomas N. DMSO efficiently down regulates pluripotency genes in human embryonic stem cells during definitive endoderm derivation and increases the proficiency of hepatic differentiation. PLoS One. 2015;10:e0117689.

Darling D, Tavassoli M, Linskens MH, Farzaneh F. DMSO induced modulation of c-myc steady-state RNA levels in a variety of different cell lines. Oncogene. 1989;4:175–9.

Flynn TJ, Ferguson MS. Multiendpoint mechanistic profiling of hepatotoxicants in HepG2/C3A human hepatoma cells and novel statistical approaches for development of a prediction model for acute hepatotoxicity. Toxicol in Vitro. 2008;22:1618–31.

Gerets HH, Tilmant K, Gerin B, Chanteux H, Depelchin BO, Dhalluin S, Atienzar FA. Characterization of primary human hepatocytes, HepG2 cells, and HepaRG cells at the mRNA level and CYP activity in response to inducers and their predictivity for the detection of human hepatotoxins. Cell Biol Toxicol. 2012;28:69–87.

Gieseck 3rd RL, Hannan NR, Bort R, Hanley NA, Drake RA, Cameron GW, Wynn TA, Vallier L. Maturation of induced pluripotent stem cell derived hepatocytes by 3D-culture. PLoS One. 2014;9:e86372.

Gripon P, Rumin S, Urban S, Le Seyec J, Glaise D, Cannie I, Guyomard C, Lucas J, Trepo C, Guguen-Guillouzo C. Infection of a human hepatoma cell line by hepatitis B virus. Proc Natl Acad Sci U S A. 2002;99:15655–60.

Guillouzo A, Corlu A, Aninat C, Glaise D, Morel F, Guguen-Guillouzo C. The human hepatoma HepaRG cells: a highly differentiated model for studies of liver metabolism and toxicity of xenobiotics. Chem Biol Interact. 2007;168:66–73.

Hart SN, Li Y, Nakamoto K, Subileau EA, Steen D, Zhong XB. A comparison of whole genome gene expression profiles of HepaRG cells and HepG2 cells to primary human hepatocytes and human liver tissues. Drug metabolism and disposition: the biological fate of chemicals. 2010;38:988–94.

Hewitt NJ, Lechon MJ, Houston JB, Hallifax D, Brown HS, Maurel P, Kenna JG, Gustavsson L, Lohmann C, Skonberg C, et al. Primary hepatocytes: current understanding of the regulation of metabolic enzymes and transporter proteins, and pharmaceutical practice for the use of hepatocytes in metabolism, enzyme induction, transporter, clearance, and hepatotoxicity studies. Drug Metab Rev. 2007;39:159–234.

Holmgren G, Sjogren AK, Barragan I, Sabirsh A, Sartipy P, Synnergren J, Bjorquist P, Ingelman-Sundberg M, Andersson TB, Edsbagge J. Long-term chronic toxicity testing using human pluripotent stem cell-derived hepatocytes. Drug metabolism and disposition: the biological fate of chemicals. 2014;42:1401–6.

Irizarry RA, Hobbs B, Collin F, Beazer-Barclay YD, Antonellis KJ, Scherf U, Speed TP. Exploration, normalization, and summaries of high density oligonucleotide array probe level data. Biostatistics (Oxford, England). 2003;4:249–64.

Isom HC, Secott T, Georgoff I, Woodworth C, Mummaw J. Maintenance of differentiated rat hepatocytes in primary culture. Proc Natl Acad Sci U S A. 1985;82:3252–6.

Jacob SW, Herschler R. Pharmacology of DMSO. Cryobiology. 1986;23:14–27.

Kennedy RH. In vitro toxicology testing: it's time to report the sex of cells. Toxicol Forensic Med Open J. 2016;1:e5–8.

Koturbash I, Scherhag A, Sorrentino J, Sexton K, Bodnar W, Swenberg JA, Beland FA, Pardo-Manuel Devillena F, Rusyn I, Pogribny IP. Epigenetic mechanisms of mouse interstrain variability in genotoxicity of the environmental toxicant 1,3-butadiene. Toxicol Sci. 2011;122:448–56.

Liu J, Yoshikawa H, Nakajima Y, Tasaka K. Involvement of mitochondrial permeability transition and caspase-9 activation in dimethyl sulfoxide-induced apoptosis of EL-4 lymphoma cells. Int Immunopharmacol. 2001;1:63–74.

Liu Y, Flynn TJ, Xia M, Wiesenfeld PL, Ferguson MS. Evaluation of CYP3A4 inhibition and hepatotoxicity using DMSO-treated human hepatoma HuH-7 cells. Cell Biol Toxicol. 2015;31:221–30.

Lu J, Einhorn S, Venkatarangan L, Miller M, Mann DA, Watkins PB, LeCluyse E. Morphological and functional characterization and assessment of iPSC-derived hepatocytes for in vitro toxicity testing. Toxicol Sci. 2015;147:39–54.

Maliepaard M, Scheffer GL, Faneyte IF, van Gastelen MA, Pijnenborg AC, Schinkel AH, van De Vijver MJ, Scheper RJ, Schellens JH. Subcellular localization and distribution of the breast cancer resistance protein transporter in normal human tissues. Cancer Res. 2001;61:3458–64.

Mann DA. Human induced pluripotent stem cell-derived hepatocytes for toxicology testing. Expert Opin Drug Metab Toxicol. 2015;11:1–5.

Medine CN, Lucendo-Villarin B, Storck C, Wang F, Szkolnicka D, Khan F, Pernagallo S, Black JR, Marriage HM, Ross JA, et al. Developing high-fidelity hepatotoxicity models from pluripotent stem cells. Stem cells translational medicine. 2013;2:505–9.

Nagamoto Y, Tashiro K, Takayama K, Ohashi K, Kawabata K, Sakurai F, Tachibana M, Hayakawa T, Furue MK, Mizuguchi H. The promotion of hepatic maturation of human pluripotent stem cells in 3D co-culture using type I collagen and Swiss 3 T3 cell sheets. Biomaterials. 2012;33:4526–34.

Nakabayashi H, Taketa K, Miyano K, Yamane T, Sato J. Growth of human hepatoma cells lines with differentiated functions in chemically defined medium. Cancer Res. 1982;42:3858–63.

Raab S, Klingenstein M, Liebau S, Linta L. A comparative view on human somatic cell sources for iPSC generation. Stem Cells Int. 2014;2014:768391.

Richert L, Liguori MJ, Abadie C, Heyd B, Mantion G, Halkic N, Waring JF. Gene expression in human hepatocytes in suspension after isolation is similar to the liver of origin, is not affected by hepatocyte cold storage and cryopreservation, but is strongly changed after hepatocyte plating. Drug metabolism and disposition: the biological fate of chemicals. 2006;34:870–9.

Ringner M. What is principal component analysis? Nat Biotechnol. 2008;26:303–4.

Sakai Y, Jiang J, Kojima N, Kinoshita T, Miyajima A. Enhanced in vitro maturation of fetal mouse liver cells with oncostatin M, nicotinamide, and dimethyl sulfoxide. Cell Transplant. 2002;11:435–41.

Santos NC, Figueira-Coelho J, Martins-Silva J, Saldanha C. Multidisciplinary utilization of dimethyl sulfoxide: pharmacological, cellular, and molecular aspects. Biochem Pharmacol. 2003;65:1035–41.

Sassa S, Sugita O, Galbraith RA, Kappas A. Drug metabolism by the human hepatoma cell, Hep G2. Biochem Biophys Res Commun. 1987;143:52–7.

Schwartz RE, Fleming HE, Khetani SR, Bhatia SN. Pluripotent stem cell-derived hepatocyte-like cells. Biotechnol Adv. 2014;32:504–13.

Si-Tayeb, K., Noto, F.K., Nagaoka, M., Li, J., Battle, M.A., Duris, C., North, P.E., Dalton, S., and Duncan, S.A. (2010). Highly efficient generation of human hepatocyte-like cells from induced pluripotent stem cells. Hepatology (Baltimore, Md.) 51, 297–305.

Singh VK, Kumar N, Kalsan M, Saini A, Chandra R. Mechanism of induction: induced pluripotent stem cells (iPSCs). Journal of stem cells. 2015;10:43–62.

Sirenko O, Hesley J, Rusyn I, Cromwell EF. High-content assays for hepatotoxicity using induced pluripotent stem cell-derived cells. Assay Drug Dev Technol. 2014;12:43–54.

Srinivas S, Sironmani TA, Shanmugam G. Dimethyl sulfoxide inhibits the expression of early growth-response genes and arrests fibroblasts at quiescence. Exp Cell Res. 1991;196:279–86.

Sullivan, G.J., Hay, D.C., Park, I.H., Fletcher, J., Hannoun, Z., Payne, C.M., Dalgetty, D., Black, J.R., Ross, J.A., Samuel, K., et al. (2010). Generation of functional human hepatic endoderm from human induced pluripotent stem cells. Hepatology (Baltimore, Md.) 51, 329–335.

Sun C, Wilson GS, Fan JG, Qiao L. Potential applications of induced pluripotent stem cells (iPSCs) in hepatology research. Current Stem Cell Research & Therapy. 2015;10:208–15.

Suter-Dick L, Alves PM, Blaauboer BJ, Bremm KD, Brito C, Coecke S, Flick B, Fowler P, Hescheler J, Ingelman-Sundberg M, et al. Stem cell-derived systems in toxicology assessment. Stem Cells Dev. 2015;24:1284–96.

Takahashi K, Yamanaka S. Induction of pluripotent stem cells from mouse embryonic and adult fibroblast cultures by defined factors. Cell. 2006;126:663–76.

Takayama K, Kawabata K, Nagamoto Y, Kishimoto K, Tashiro K, Sakurai F, Tachibana M, Kanda K, Hayakawa T, Furue MK, et al. 3D spheroid culture of hESC/hiPSC-derived hepatocyte-like cells for drug toxicity testing. Biomaterials. 2013;34:1781–9.

Tong W, Cao X, Harris S, Sun H, Fang H, Fuscoe J, Harris A, Hong H, Xie Q, Perkins R, et al. ArrayTrack—supporting toxicogenomic research at the U.S. Food and Drug

Administration National Center for toxicological research. Environ Health Perspect. 2003;111:1819–26.

Wang B, Jakus AE, Baptista PM, Soker S, Soto-Gutierrez A, Abecassis MM, Shah RN, Wertheim JA. Functional maturation of induced pluripotent stem cell hepatocytes in extracellular matrix-a comparative analysis of bioartificial liver microenvironments. Stem cells translational medicine. 2016;5:1257–67.

Ward Jr JH. Hierarchical grouping to optimize an objective function. J Am Stat Assoc. 1963;58:236–44.

Ware BR, Berger DR, Khetani SR. Prediction of drug-induced liver injury in Micropatterned Co-cultures containing iPSC-derived human hepatocytes. Toxicol Sci. 2015;145:252–62.

Xu JJ, Diaz D, O'Brien PJ. Applications of cytotoxicity assays and pre-lethal mechanistic assays for assessment of human hepatotoxicity potential. Chem Biol Interact. 2004;150:115–28.